N O T I C E

THIS DOCUMENT HAS BEEN REPRODUCED FROM MICROFICHE. ALTHOUGH IT IS RECOGNIZED THAT CERTAIN PORTIONS ARE ILLEGIBLE, IT IS BEING RELEASED IN THE INTEREST OF MAKING AVAILABLE AS MUCH INFORMATION AS POSSIBLE

NASA Technical Memorandum 81628

Theoretical Model Applicable to the Experimental Determination of Surface Anchoring Energies of Nematic Liquid Crystals

(NASA-TM-81628) THEORETICAL MODEL APPLICABLE TO THE EXPERIMENTAL DETERMINATION OF SURFACE ANCHORING ENERGIES OF NEMATIC LIQUID CRYSTALS M.S. Thesis (NASA) 34 p HC A03/MF A01 CSCL 20B G3/70

N81-12817

Unclas 29326

Edwin G. Wintucky
Lewis Research Center
Cleveland, Ohio

November 1980

DEC1980
RECEIVED
NASA STI FACILITY
ACCESS DEPT.

NASA

INTRODUCTION

The chemical and physical interactions causing molecular orientation at liquid crystal-solid interfaces are a subject of fundamental physical interest. They are also important for practical applications in liquid crystal display devices. The successful operation of most electrooptic liquid crystal displays requires a well defined alignment of the liquid crystal molecules at the substrate surface. Special chemical or mechanical treatments of the substrate surface are required to obtain the alignment (Ref. 1).

The optical behavior of an electrooptic liquid crystal display is controlled by an applied electric field. A typical display geometry consists of a thin nematic layer (10-20 μm thick) sandwiched between two parallel surfaces, which have been treated to produce alignment. In the absence of electric (or magnetic) fields, the equilibrium bulk orientation is determined by the elastic response of the liquid crystal to the interaction forces at the surface boundaries. The orientation of a nematic liquid crystal is conventionally described by the director, $\hat{n}$, a unit vector representing the average orientation of the long molecular axes in a local region of space whose dimensions are small compared to the long range of the ordering forces present in a liquid crystal. An ordered nematic liquid crystal behaves optically like a uniaxial single crystal with the optic axis parallel to the director $\hat{n}$. For liquid crystals with positive dielectric anisotropy, the application of an electric field tends to reorient the molecules along the field direction.

The onset of reorientation occurs at a critical voltage, producing a sharp transition in the optical properties.

Among the electrooptical qualities desired for good device performance are sharpness of transition and transparency. These qualities are critically influenced by the direction and uniformity of the initial surface alignment and by the strength of interaction (pinning strength) between the surface forces and the liquid crystal molecules (Ref. 2). A measure of the pinning strength is the anchoring energy. Quantitative evaluation of the anchoring energies for various surface treatments, types of alignment and different liquid crystal materials is needed for a better understanding of the diverse factors contributing to surface alignment and could be useful to the development of display technology.

The most commonly used model for the surface energy (Ref. 2), reflecting the anisotropic nature of the surface interactions, has the form

$$\omega = W \sin^2(\Delta\theta) \qquad (1)$$

where ω (ergs/cm^2) is the energy required to rotate the director away from its preferred surface orientation (called the "easy direction") through a small angle $\Delta\theta$. The coefficient W in this expression is the surface anchoring energy. Equation (1) has been used in measurements of surface energies corresponding to rotations of the director both in a vertical direction away from the plane of the substrate and in the plane of the substrate. Extremes of observed anchoring energies, corresponding to different surface treatments, range from about 10^{-4} ergs/cm^2 (weak anchoring) for rotations in a vertical direction up to about one erg/cm^2 (strong anchoring) for rotations in the plane of the substrate (Ref. 2).

Another parameter sometimes used to characterize surface energies is "extrapolation length" (Ref. 3, p. 74), whose magnitude is on the order of K/W, where K is an elastic constant of the liquid crystal (generally about 10^{-6} dynes). The extrapolation length defines an effective sample thickness when a distortion has been imposed on the bulk orientation and can be regarded as a measure of the continuation into the substrate of the angular variation of the director. For strong anchoring conditions, in which the surface energies are comparable to or larger than the interaction energies between molecules, the extrapolation length is on the order of or smaller than average molecular dimensions ($\lesssim$100 A) and for all practical purposes is essentially zero. For weak anchoring conditions, the surface energies are much smaller than the intermolecular interaction energies. Then the extrapolation length is much larger than the molecular dimensions and can be as high as 100 μm.

Only a few methods exist for the experimental determination of surface anchoring energies. In one of these methods (Ref. 4), quantitative estimates of anchoring energies have been obtained from a combination of optical analyses of the variation in director orientation across surface disclination lines and measurements of the equilibrium line widths. Surface disclination lines are a common defect observed in liquid crystals and are lines of discontinuity in the molecular orientation attached to the substrate surface. In a second method, analysis of the wall effects on the magnetic Freederickse transition in a homeotropically aligned nematic cell have been used to evaluate anchoring energies for substrates treated with various surfactants (Ref. 5). In yet another method,

anchoring energies were determined in twisted nematic cells from measurements of the director rotation caused by application of a magnetic field (Ref. 6).

A new method for evaluating surface anchoring energies from measurements of the director orientation at the surface boundary of a nematic liquid crystal cell has been presented recently by Rivière, Lévy and Guyon (Ref. 7). The theoretical and experimental results of Rivière, Lévy and Guyon (RLG) are briefly reviewed below.

The sample used in the RLG experiment consisted of a slightly wedge-shaped nematic liquid crystal cell formed by two nearly parallel glass plates. The sample geometry is shown in Figure 1.

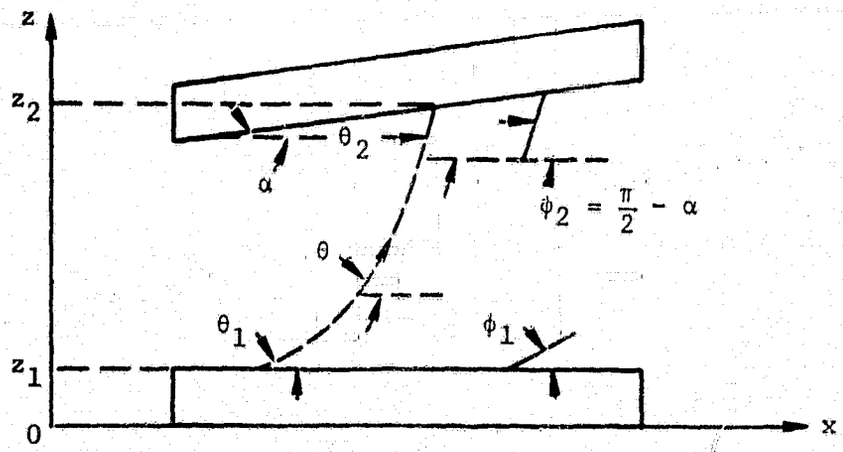

Figure 1. Liquid crystal sample geometry used for determination of surface anchoring energy from tilt angle measurement.

The angles ϕ_1 and ϕ_2 are the easy directions of alignment and represent what the tilt angles would be for each surface alone. The angles θ_1 and θ_2 are the actual tilt angles and are distortions induced by the opposite surface. The small wedge angle α in the RLG study was 18 minutes of arc. The upper surface was treated with an organosilane to

produce a strong homeotropic alignment ($\phi_2 \sim 90^o$). The lower surface was coated with an obliquely deposited SiO film which provided an easy direction of $\phi_1 \sim 30^o$. The angle θ was the angle formed by the director $\hat{n}$ and the X-axis. Rotations of the director were assumed confined to the XOZ plane.

To derive an expression relating surface anchoring energy to the tilt angle θ_1 and sample thickness d, RLG started with the free energy density as given by the isotropic elastic continuum theory for liquid crystals,

$$F_d = \frac{1}{2} K (\nabla\theta)^2 \tag{2}$$

To simplify calculations, the one-constant approximation was assumed, in which the liquid crystal is considered as an isotropic elastic medium whose elastic properties are represented by a single elastic constant, K. For this free energy density, the Euler-Lagrange equation for minimization of the total bulk free energy is simply Laplace's equation, $\nabla^2\theta = 0$. Because of the small wedge angle α, it was also assumed that the variation of the director angle θ in the X-direction was much smaller than in the Z-direction, viz., $\frac{\partial\theta}{\partial x} << \frac{\partial\theta}{\partial z}$. For this assumption $\nabla^2\theta = \frac{\partial^2\theta}{\partial z^2} = 0$. Integration of the one dimensional Laplace equation gives

$$\theta = az + \theta_o \tag{3}$$

where $a = \frac{\partial\theta}{\partial z}$. For a given x, $a = \frac{\theta_2 - \theta_1}{d}$ where d is the sample thickness at that point. The surface energy at the lower surface (subscript 1) was assumed to be given by

$$\omega_{S1} = W_1 \sin^2(\theta_1 - \phi_1) \tag{4}$$

Substitition of Eq. (4) into the equation representing the balance between the surface and elastic torques,

$$\frac{d\omega_{S1}}{d\theta} = K\left(\frac{\partial\theta}{\partial z}\right)_{z=z_1} \tag{5}$$

resulted in the following expression for the surface anchoring energy

$$W_1 = \frac{K(\theta_2 - \theta_1)}{d \sin[2(\theta_1 - \phi_1)]} \tag{6}$$

To enable evaluation of W_1 from experimental measurements of the tilt angle θ_1 and sample thickness d only, some additional approximations were made. One approximation was that $\frac{\theta_2 - \theta_1}{d} \cong \frac{\phi_2 - \phi_1}{d} = \frac{\Delta\phi}{d}$ and that $\Delta\phi$ was constant over the region of measurement. Also for small angles $(\theta_1 - \phi_1)$, it was assumed that $\sin[2(\theta_1 - \phi_1)] \cong 2(\theta_1 - \phi_1)$. Using tilt angles, θ_1' and θ_1'', and the corresponding sample thicknesses, d' and d'', measured at two locations along the lower surface, Eq. (6) can be rewritten as

$$W_1 = \frac{K(\Delta\phi)}{2(\theta_1' - \theta_1'')}\left(\frac{1}{d'} - \frac{1}{d''}\right) \tag{7}$$

The tilt angles were deduced to within $\pm 0.3^{\circ}$ from reflectivity measurements at the critical angle of parallel polarized light from a laser light source (Refs. 7,8). Using an approximate value of $K \sim 10^{-6}$ erg-cm, RLG reported a calculated value for W_1 of $(2.1 \pm 0.8)\times 10^{-3}$ ergs/cm^2, which generally agreed with previously reported values of the surface anchoring energy for the same surface treatment.

The purpose of this thesis is to extend and generalize the theory presented by RLG to include non-equal elastic constants and a two

dimensional variation of the director orientation. The sample geometry and parameters are the same as defined by Figure 1. The sequence of presentation is as follows. First, there will be a very brief discussion of relevant aspects of the elastic continuum theory for nematic liquid crystals. Then, an analytical solution to the one-dimensional problem allowing for elastic anisotropy, i.e., assuming non-equal elastic constants, will be presented and discussed. This will be followed by a special solution for the two-dimensional problem, appropriate for the slightly perturbed one-dimensional geometry representing the wedge-shaped liquid crystal sample. Next, a comparison will be made between the surface anchoring energies obtained using the one-dimensional, elastically isotropic approximation and the two solutions for elastic anisotropy presented here. Finally, an experiment for measuring surface anchoring energies using the analytic solution for the one-dimensional case will be proposed.

ELASTIC CONTINUUM THEORY

A number of large scale phenomena involving the response of the bulk liquid crystal to external disturbances can be successfully described by the elastic continuum theory (Ref. 3, Chap. 3; Ref. 9, Chap. 8), in which the liquid crystal is treated as a continuous elastic medium. In the absence of applied electric or magnetic fields, the thermodynamic equilibrium state is determined solely by the elastic response of the bulk liquid crystal to the surface interaction forces at the walls of its container. The surface forces induce a static distortion of the director orientation.

The starting point for calculations is the equation for the elastic free energy density, expressed in terms of the director field, $\hat{n}(\vec{r})$. The elastic free energy density is given by

$$F_d = \frac{1}{2}\left\{K_1\left[\nabla\cdot\hat{n}(\vec{r})\right]^2 + K_2\left[\hat{n}(\vec{r})\cdot\nabla\times\hat{n}(\vec{r})\right]^2 + K_3\left[\hat{n}(\vec{r})\times(\nabla\times\hat{n}(\vec{r}))\right]^2\right\} \qquad (8)$$

Here K_1, K_2 and K_3 are the Franck elastic constants and correspond to the three basic types of distortion for a nematic liquid crystal, namely, splay, twist and bend, respectively. The basic problem in applications of the elastic continuum theory is to determine that director configuration which minimizes the total free energy. The total free energy is given by

$$F = F_B + F_S$$

$$= \int_{\substack{\text{Volume}\\ \text{of sample}}} F_d\left(\hat{n}, \frac{\partial\hat{n}}{\partial x_i}, x_i\right) dv + F_S \qquad (i = 1,2,3) \qquad (9)$$

where F_B is the total bulk elastic free energy and F_S is the total surface energy. The equilibrium conditions are determined by minimizing the total free energy with respect to all variations of the director $\hat{n}(\vec{r})$ subject to the constraint $\hat{n}\cdot\hat{n} = 1$. In actual calculations it is more convenient to write $\hat{n}$ in terms of appropriate polar angles and minimize F with respect to all variations of these angles.

For the sample geometry shown in Figure 1, all rotations of the director are assumed to take place only in the XOZ plane. There is then only one polar angle, θ, as defined in Figure 1. In terms of θ, the components of $\hat{n}$ are

$$n_x = \hat{n}\cdot\hat{e}_x = \cos\theta$$

$$n_y = \hat{n}\cdot\hat{e}_y = 0$$

$$n_z = \hat{n}\cdot\hat{e}_z = \sin\theta$$

where $\hat{e}_x$, $\hat{e}_y$, $\hat{e}_z$ are the unit vectors for the Cartesian coordinate system. By direct calculation

$$\nabla\cdot\hat{n} = -\sin\theta\theta_x + \cos\theta\theta_z$$

and

$$\nabla \times \hat{n} = -(\cos\theta\theta_x + \sin\theta\theta_z)\hat{e}_y$$

where

$$\theta_x = \frac{\partial\theta}{\partial x}, \quad \theta_z = \frac{\partial\theta}{\partial z}$$

Then

$$(\nabla\cdot\hat{n})^2 = (\sin\theta\theta_x - \cos\theta\theta_z)^2$$

$$\hat{n}\cdot\nabla \times \hat{n} = 0$$

$$\left[\hat{n} \times (\nabla \times \hat{n})\right]^2 = (\cos\theta\theta_x + \sin\theta\theta_z)^2$$

The free energy density is

$$F_d = \frac{1}{2}\left(g_1\theta_x^2 + g_2\theta_x\theta_z + g_3\theta_z^2\right) \tag{10}$$

where

$$\begin{aligned} g_1 &= K_1\sin^2\theta + K_3\cos^2\theta \\ g_2 &= 2(K_1 - K_3)\sin\theta\cos\theta \\ g_3 &= K_1\cos^2\theta + K_3\sin^2\theta \end{aligned} \tag{11}$$

In the one-constant approximation where $K = K_1 = K_3$, Eq. (10) reduces to the F_d given by Eq. (2).

Using Eq. (10) for the elastic free energy density, Eq. (9) for the total free energy can be written

$$F = \iiint F_d(\theta,\theta_x,\theta_z)dxdydz + \sum_{i=1,2} \iint \omega_i da_i \tag{12}$$

where

$$\omega_i = W_i \sin^2(\theta_i - \phi_i) \tag{13}$$

and da_i is an element of area on the ith surface.

The minimization of F requires that

$$\delta F = \iiint \delta F_d(\theta,\theta_x,\theta_z)dxdydz + \sum_{i=1,2} \iint \delta\omega_i da_i = 0 \tag{14}$$

for arbitrary variations $\delta\theta$ in the director angle θ. According to the calculus of variations, the variation δF_d can be written as

$$\delta F_d(\theta,\theta_x,\theta_z) = \frac{\partial F_d}{\partial \theta}\,\delta\theta + \frac{\partial F_d}{\partial \theta_x}\,\delta\theta_x + \frac{\partial F_d}{\partial \theta_z}\,\delta\theta_z$$

$$= \frac{\partial F_d}{\partial \theta}\,\delta\theta + \frac{\partial F_d}{\partial \theta_x}\frac{\partial}{\partial x}(\delta\theta) + \frac{\partial F_d}{\partial \theta_z}\frac{\partial}{\partial z}(\delta\theta)$$

$$= \left[\frac{\partial F_d}{\partial \theta} - \frac{\partial}{\partial x}\left(\frac{\partial F_d}{\partial \theta_x}\right) - \frac{\partial}{\partial z}\left(\frac{\partial F_d}{\partial \theta_z}\right)\right]\delta\theta + \frac{\partial}{\partial x}\left(\frac{\partial F_d}{\partial \theta_x}\,\delta\theta\right) + \frac{\partial}{\partial z}\left(\frac{\partial F_d}{\partial \theta_z}\,\delta\theta\right) \tag{15}$$

where $\delta\theta_x = \frac{\partial}{\partial x}(\delta\theta)$ and $\delta\theta_z = \frac{\partial}{\partial z}(\delta\theta)$.

The variation in the total free energy is then

$$\delta F = \iiint \left[\frac{\partial F_d}{\partial \theta} - \frac{\partial}{\partial x}\left(\frac{\partial F_d}{\partial \theta_x}\right) - \frac{\partial}{\partial z}\left(\frac{\partial F_d}{\partial \theta_z}\right)\right] \delta\theta \, dxdydz$$
$$+ \iiint \left[\frac{\partial}{\partial x}\left(\frac{\partial F_d}{\partial \theta_x}\,\delta\theta\right) + \frac{\partial}{\partial z}\left(\frac{\partial F_d}{\partial \theta_z}\,\delta\theta\right)\right] dxdydz + \sum_{i=1,2} \iint \delta\omega_i da_i = 0 \tag{16}$$

where $\delta\omega_i = \frac{\partial \omega_i}{\partial \theta}\,\delta\theta\Big|_{\theta=\theta_i}$.

DeGennes has shown (Ref. 3, pp. 73-76) that when the surface forces are strong enough to orient the director $\hat{n}$ in a well-defined direction ("easy direction") at the surface, the extrapolation length is on the order of molecular dimensions. It then suffices to neglect the surface terms and to minimize the bulk free energy term only, with fixed boundary conditions for $\hat{n}$. This is a common practice in most calculations using the elastic continuum theory. In that case one would consider only the first integral in Eq. (16). As a condition for local bulk equilibrium, one has the familiar Euler-Lagrange equation,

$$\frac{\partial F_d}{\partial \theta} - \frac{\partial}{\partial x}\left(\frac{\partial F_d}{\partial \theta_x}\right) - \frac{\partial}{\partial z}\left(\frac{\partial F_d}{\partial \theta_z}\right) = 0 \tag{17}$$

In the case considered here, however, surface energy plays an important role. We are looking at the influence of one surface, manifesting itself in torques transmitted through the liquid crystal, in modifying the orientation of the director at the opposite surface. The surface

terms cannot be ignored. In addition to Eq. (17), which expresses the condition for local equilibrium in the bulk, we have the following condition for mechanical equilibrium at the substrate surfaces.

$$\iiint \left[\frac{\partial}{\partial x}\left(\frac{\partial F_d}{\partial \theta_x}\,\delta\theta\right) + \frac{\partial}{\partial z}\left(\frac{\partial F_d}{\partial \theta_z}\,\delta\theta\right)\right] dx\,dy\,dz + \sum_{i=1,2} \iint \left[\frac{\partial \omega_i}{\partial \theta}\,\delta\theta\right]_{z=z_i} dx_i = 0 \tag{18}$$

As will be seen, in subsequent applications to the one- and two-dimensional cases, Eq. (18) introduces in a natural way the boundary conditions expressing the balance between surface energy torques $\left.\frac{\partial \omega_i}{\partial \theta}\right|_{\theta=\theta_i}$ exerted on the liquid crystal and the elastic torques exerted by the liquid crystal.

VARIATION IN ONE DIMENSION

We consider first the case where it is assumed that variations of the director angle θ in the X-direction can be neglected in the calculation of the equilibrium conditions, i.e., $\theta_x << \theta_z$. This assumption is equivalent to taking the two surfaces to be parallel. Equation (10) for the free energy density is then

$$F_d(\theta,\theta_z) = \frac{1}{2}\, g_3 \theta_z^2 \tag{19}$$

where $g_3 = K_1\cos^2\theta + K_3\sin^2\theta$. The Euler-Lagrange equation for bulk equilibrium is

$$\frac{\partial F_d}{\partial \theta} - \frac{\partial}{\partial z}\left(\frac{\partial F_d}{\partial \theta_z}\right) = 0 \tag{20}$$

Substitution of Eq. (19) into Eq. (20) gives for the Euler-Lagrange equation,

$$\frac{1}{2} g_{3\theta}\theta_z^2 + g_3\theta_{zz} = 0 \tag{21}$$

where $g_{3\theta} = \frac{\partial g_3}{\partial \theta}$ and $\theta_{zz} = \frac{\partial^2 \theta}{\partial z^2}$. With z being the only independent variable, θ_z and θ_{zz} are total derivatives. Eq. (21) is an ordinary second order differential equation which can be integrated directly as follows. First multiply by θ_z. Then

$$\frac{1}{2} g_{3\theta}\theta_z^3 + g_3\theta_z\theta_{zz} = \frac{d}{dz}\left(\frac{1}{2} g_3\theta_z^2\right) \tag{22}$$

$$= \frac{d}{dz}(F_d)$$

$$= 0$$

The free energy density is thus a constant which can be evaluated in terms of the boundary conditions as follows. Let $F_d = C$. Then

$$\frac{d\theta}{dz} = \left(\frac{2C}{g_3}\right)^{1/2} \tag{23}$$

Integration of Eq. (23) gives

$$\sqrt{2C}\,(z_2 - z_1) = \int_{\theta_1}^{\theta_2} g_3^{1/2} d\theta \tag{24}$$

Let $d = z_2 - z_1$ be the sample thickness and

$$E_1(\theta_1,\theta_2) = \int_{\theta 1}^{\theta_2} g_3^{1/2} d\theta$$

$$= \int_{\theta_1}^{\theta_2} (K_1 \cos^2\theta + K_3 \sin^2\theta)^{1/2} d\theta \qquad (25)$$

$E_1(\theta_1,\theta_2)$ is an elliptic type integral and is readily evaluated, given θ_1, θ_2, K_1 and K_3. The subscript 1 in $E_1(\theta_1,\theta_2)$ refers to the one-dimensional variation of θ. The free energy density is then

$$F_d = \frac{1}{2d^2} \left[E_1(\theta_1,\theta_2)\right]^2 = C \qquad (26)$$

For two parallel surfaces, the elastic free energy density given by Eq. (26) is constant throughout the sample. For the slightly wedge-shaped sample, calculation of the equilibirum conditions based on the assumption that θ_x can be neglected indicates that F_d remains constant (or approximately so). This implies that at a given location x, where the sample thickness is d, θ_1 and θ_2 should assume values such that Eq. (26) is satisfied.

The surface terms in the variational calculation, Eq. (18), give the equilibrium conditions for the balance of torques at the surface. From the balance of torque equation, one then obtains an expression relating surface anchoring energy to measurable parameters such as sample thickness d and tilt angles θ_1 and θ_2.

Consider the lower surface, $z = z_1$. The variation in surface energy, $\delta\omega_1 = \frac{\partial\omega_1}{\partial\theta}\,\delta\theta\Big|_{\theta=\theta_1}$, is

$$\delta\omega_1 = 2W_1 \sin(\theta - \phi_1)\cos(\theta - \phi_1)\delta\theta\Big|_{\theta=\theta_1}$$

$$= W_1 \sin 2(\theta - \phi_1)\delta\theta\Big|_{\theta=\theta_1} \tag{27}$$

For the one-dimensional case, where $\frac{\partial F_d}{\partial \theta_x} = 0$, the first integral in Eq. (18) is

$$\int_{z_1}^{z_2} \frac{\partial}{\partial z}\left(\frac{\partial F_d}{\partial \theta_z}\,\delta\theta\right) dz = \left[\frac{\partial F_d}{\partial \theta_z}\,\delta\theta\right]_{z_1}^{z_2} \tag{28}$$

Combining the lower limit of Eq. (28) with the variation $\delta\omega_1$ given by Eq. (27), one obtains the following equilibrium condition expressing the balance of torques at the lower surface,

$$-\frac{\partial F_d}{\partial \theta_z}\Big|_{z=z_1} + W_1 \sin\left[2(\theta - \phi_1)\right]\Big|_{z=z_1} = 0 \tag{29}$$

From Eqs. (19) and (26),

$$\frac{\partial F_d}{\partial \theta_z} = g_3\theta_z = \frac{\sqrt{g_3}}{d}\,E_1(\theta_1,\theta_2) \tag{30}$$

The anchoring energy W_1 at the lower surface is then

$$W_1 = \frac{(g_3)^{1/2}_{\theta=\theta_1} E_1(\theta_1,\theta_2)}{d \sin\left[2(\theta_1 - \theta_1)\right]}$$

$$= \frac{(K_1\cos^2\theta_1 + K_3\sin^2\theta_1)^{1/2}\; E_1(\theta_1,\theta_2)}{d \sin\left[2(\theta_1 - \phi_1)\right]} \tag{31}$$

In the one-constant approximation where $K = K_1 = K_3$, $g_3^{1/2} = K^{1/2}$ and $E(\theta_1,\theta_2) = K^{1/2}(\theta_2 - \theta_1)$. Eq. (31) is then identical to Eq. (6). An expression for the surface anchoring energy W_2 at the upper surface can be obtained in a similar manner.

VARIATION IN TWO DIMENSIONS

For variations of the director orientation angle θ in both the x and z directions, the free energy density is given by Eq. (10) as

$$F_d(\theta,\theta_x,\theta_z) = \frac{1}{2}(g_1\theta_x + g_2\theta_x\theta_z^2 + g_3\theta_z^2) \tag{10}$$

where g_1, g_2 and g_3 are the functions of θ only defined by Eq. (11). The total free energy, elastic and surface, is given by Eq. (12) as

$$F = \iiint F_d(\theta,\theta_x,\theta_z)dxdydz + \sum_{i=1,2} \iint \omega_i da_i \tag{12}$$

The Euler-Lagrange equation representing the bulk equilibrium condition is given by Eq. (17) as

$$\frac{\partial F_d}{\partial \theta} - \frac{\partial}{\partial x}\left(\frac{\partial F_d}{\partial \theta_x}\right) - \frac{\partial}{\partial z}\left(\frac{\partial F_d}{\partial \theta_z}\right) = 0 \tag{17}$$

Upon substitution of Eq. (10) into Eq. (17), the Euler-Lagrange equation becomes

$$f(\theta,\theta_x,\theta_z,\theta_{xx},\theta_{xz},\theta_{zz}) = \frac{1}{2}(g_{1\theta}\theta_x^2 + g_{2\theta}\theta_x\theta_z + g_{3\theta}\theta_z^2)$$

$$+ (g_1\theta_{xx} + g_2\theta_x\theta_z + g_3\theta_{zz}) = 0 \tag{32}$$

where $g_{i\theta} = \frac{\partial g_i}{\partial \theta}$ $(i = 1,2,3)$, $\theta_{xx} = \frac{\partial^2 \theta}{\partial x^2}$, $\theta_{xz} = \frac{\partial^2 \theta}{\partial x \partial z}$ and $\theta_{zz} = \frac{\partial^2 \theta}{\partial z^2}$.

Eq. (32) is a "quasi-linear" second order partial differential equation, so called because of being linear in the highest order derivatives. A general solution to this equation was not found in the literature. Attempts to obtain such a solution by systematic or ad hoc methods were unsuccessful (Ref. 10).

A special solution to Eq. (32), similar to the solution to the one-dimensional Euler-Lagrange equation, Eq. (20), can be derived. This "linearized" solution is appropriate for the slightly wedge-shaped sample geometry, which is only a very small departure from the one-dimensional parallel surface geometry.

An insight into how to approach a solution can be gotten by looking back to the one-dimensional case. For the two surfaces parallel, the calculated free energy density, F_d, was found to be constant throughout the sample. This was an exact result. The same calculation was assumed approximately valid for the slightly wedge-shaped geometry with the implied result that the free energy density remained approximately constant over the dimensions of the sample. In the one-elastic constant approximation, which gives qualitatively the same results as $K_1 \neq K_3$, $F_d = \frac{1}{2} K \theta_z^2$ with $\theta_z = \frac{\theta_2 - \theta_1}{d}$. The difference in thickness between two points along the sample is $\Delta d = \tan \alpha \, \Delta x = \frac{d}{x} \Delta x$. For $\tan \alpha << 1$, $\Delta d << \Delta x$. Thus d varies very slowly with x and consequently so do θ_z and F_d. Therefore, for $\frac{x}{d} >> 1$, the assumption that the free energy density is constant over the dimensions of the sample is a reasonably good approximation.

Although variations of θ with both x and z will be allowed, let us assume that F_d remains constant over the volume of the sample. This assumption will enable a linear solution to Eq. (32). Let

$$F_d(\theta,\theta_x,\theta_z) = \frac{1}{2}\,(g_1\theta_x^2 + g_2\theta_x\theta_z + g_3\theta_z^2) = C \tag{33}$$

where C is a constant to be evaluated in terms of the boundary conditions.

For first order partial differential equations in which the independent variables do not appear explicitly, of which Eq. (33) is an example, Charpit's method (Ref. 11, pp. 69-73) can often be effectively applied to obtain a solution. In this case, two of Charpit's equations assume the especially simple form

$$\frac{d\theta_x}{\theta_x} = \frac{d\theta_z}{\theta_z} \tag{34}$$

where $d\theta_x$ and $d\theta_z$ are differentials. It follows immediately that

$$\theta_x = a\theta_z \tag{35}$$

where a is a constant. Substituting Eq. (35) into Eq. (33), we find $F_d(\theta,\theta_x,\theta_z) \rightarrow F_d(\theta,\theta_z)$ and

$$\begin{aligned} F_d(\theta,\theta_z) &= \frac{1}{2}\,(a^2g_1 + ag_2 + g_3)\theta_z^2 \\ &= \frac{1}{2}\,G\theta_z^2 \\ &= C \end{aligned} \tag{36}$$

where

$$G = a^2 g_1 + a g_2 + g_3 \tag{37}$$

Then

$$\theta_z = \left(\frac{2C}{G}\right)^{1/2}, \quad \theta_x = a\left(\frac{2C}{G}\right)^{1/2} \tag{38}$$

The expression for θ_z in Eq. (38) is similar in form to the result for one-dimensional case given by Eq. (23). For $a = 0$, whence $\theta_x = 0$, the results are identical. It is easily verified that the solution to Eq. (36) also satisfies the Euler-Lagrange equation, Eq. (32). For example, substitution of Eq. (38) into Eq. (32) shows for constant C that

$$\begin{aligned}
&\frac{1}{2}\left(g_{1\theta}\theta_x + g_{2\theta}\theta_x\theta_z + g_{3\theta}\theta_z\right) + \left(g_1\theta_{xx} + g_2\theta_{xz} + g_3\theta_{zz}\right) \\
&\quad = \frac{1}{2}\left(a^2 g_{1\theta} + a g_{2\theta} + g_{3\theta}\right)\left(\frac{2C}{G}\right) - \left(a^2 g_1 + a g_2 + g_3\right)\left(\frac{C}{G^2}\right)\left(\frac{\partial G}{\partial \theta}\right) \\
&\quad = \frac{C}{G}\frac{\partial G}{\partial \theta} - \frac{C}{G}\frac{\partial G}{\partial \theta} \\
&\quad = 0
\end{aligned}$$

A complete integral for θ can be obtained by integrating the total differential

$$\begin{aligned}
d\theta &= \theta_x dx + \theta_z dz \\
&= \theta_z(a\,dx + dz) \\
&= \left(\frac{2C}{G}\right)^{1/2}(a\,dx + dz)
\end{aligned} \tag{39}$$

It is convenient at this point to define a new function $s(x,z)$ where

$$s = ax + z \tag{40}$$

Then $ds = a\,dx + dz$ and

$$d\theta = \frac{\partial\theta}{\partial s}\,ds = \frac{\partial\theta}{\partial z}\,ds = \left(\frac{2C}{G}\right)^{1/2} ds \tag{41}$$

from which

$$\int_{\theta_1}^{\theta_2} G^{1/2} d\theta = (2C)^{1/2} \int_{s_1}^{s_2} ds \tag{42}$$

The introduction of the function s in Eq. (39) has in effect reduced the number of independent variables from two to one. To facilitate the integration of Eq. (42), let us look first at the geometrical significance of s. For s = constant,

$$ds = a\,dx + dz = 0 \Rightarrow \frac{dz}{dx} = -a$$

Similarly for θ constant,

$$d\theta = \theta_z(a\,dx + dz) = 0 \Rightarrow \frac{dz}{dx} = -a$$

In the XOZ plane, lines of constant s and θ are parallel straight lines with slope $-a$. If one assumes rigid anchoring at the upper surface, i.e., $\theta_2 = \phi_2$ = constant, the constant a is related directly to $\tan\alpha$, in fact, $a = -\tan\alpha$. This can be directly verified in the following simple way. At the upper surface, $\theta = \theta_2$ = constant implies that everywhere on the surface that $\nabla\theta$ is normal to the surface, where $\nabla\theta = \theta_x\hat{e}_x + \theta_z\hat{e}_z$. The unit normal to the upper surface is given by

$$\hat{N} = \sin\alpha\,\hat{e}_x - \cos\alpha\,\hat{e}_z$$

Then

$$\nabla\theta \times \hat{N} = \theta_z(a\hat{e}_x + \hat{e}_z) \times (\sin\alpha\ \hat{e}_x - \cos\alpha\ \hat{e}_z)$$

$$= \theta_z(a\cos\alpha + \sin\alpha)\hat{e}_y$$

$$= 0$$

from which $a = -\tan\alpha$. The surfaces of constant θ and s are thus planes parallel to the upper inclined surface. The gradients, which are normal to these surfaces, are related by

$$\nabla\theta = \theta_z(a\ \hat{e}_x + \hat{e}_z) = \frac{\partial\theta}{\partial s}\nabla s \tag{43}$$

Generally, θ_2 is not expected to be constant over the dimensions of the sample, even for strong homeotropic alignment at the upper surface, and most likely would vary slowly with x. For large differences between θ_1 and θ_2, the parallel planes representing the surfaces of constant θ cannot intersect both the upper and lower surfaces. Consequently, $|a| < \tan\alpha$. In the special case of rigid anchoring at the upper surface just considered, $|a|$ has a maximum value of $\tan\alpha$ (5.24×10^{-3} for $\alpha = 18$ minutes of arc). Generally, $0 < |a| < \tan\alpha$.

As in the one-dimensional case, the constant C denoting the free energy density can be evaluated in terms of the boundary conditions. Let (x_a, z_{1a}) be a point on the lower surface with tilt angle θ_{1a} and (x_a, z_{2a}) be the opposite point on the upper surface with tilt angle θ_{2a}. Integrating Eq. (42) along $ds = dz$ between these points, we obtain

$$\frac{1}{\sqrt{2C}}\int_{\theta_{1a}}^{\theta_{2a}} G^{1/2}\,d\theta = S_{2a} - S_{1a} = Z_{2a} - Z_{1a} = d_a \tag{44}$$

where d_a is the sample thickness at $x = x_a$. Let

$$E_2(\theta_1,\theta_2) = \int_{\theta_1}^{\theta_2} G^{1/2} d\theta \tag{45}$$

Like $E_1(\theta_1,\theta_2)$ in Eq. (25), $E_2(\theta_1,\theta_2)$ is an elliptic integral and can be evaluated numerically, given a, K_1, K_2, θ_1 and θ_2. The subscript 2 refers to the integral being a result of a two-dimensional analysis. With the understanding that θ_1, θ_2 and d all correspond to the same x, we drop the subscript a in Eq. (44). Combining Eq. (44) with Eq. (45), we obtain for the free energy density

$$F_d = \frac{[E_2(\theta_1,\theta_2)]^2}{2d^2} = C \tag{46}$$

For $a = 0$, $E_1 = E_2$ and Eq. (46) becomes identical to Eq. (26) for the one-dimensional case.

An alternate approach to the solution of the Euler-Lagrange equation, Eq. (32), which yields the same expression for the free energy density, Eq. (46), is the following. Because the slightly wedge-shaped sample geometry is such a small departure from the parallel surface geometry ($\tan \alpha << 1$), assume that θ can be represented by a function of a linear combination of x and z, $ax + z$, where a is on the order of $\tan \alpha$. Let $\theta = \theta(s)$ where

$$s = ax + z \tag{47}$$

Then

$$\theta_z = \frac{\partial \theta}{\partial s}\frac{\partial s}{\partial z} = \frac{\partial \theta}{\partial s}; \quad \theta_x = \frac{\partial \theta}{\partial s}\frac{\partial s}{\partial x} = a\frac{\partial \theta}{\partial s} = a\theta_z \tag{48}$$

Substitution of Eq. (48) into Eq. (10) for the free energy density gives

$$F_d\left(\theta, \frac{\partial\theta}{\partial s}\right) = \frac{1}{2} G \left(\frac{\partial\theta}{\partial s}\right)^2 \tag{49}$$

where G is the function of θ only defined by Eq. (37). Substitution of Eq. (48) into the Euler-Lagrange equation, Eq. (32), gives

$$\frac{1}{2}\frac{\partial}{\partial s}\left(\frac{\partial\theta}{\partial s}\right) + G\frac{\partial^2\theta}{\partial s^2} = 0$$

which upon multiplication by $\frac{\partial\theta}{\partial s}$ can be rewritten as

$$\frac{\partial}{\partial s}\left[\frac{1}{2} G \left(\frac{\partial\theta}{\partial s}\right)^2\right] = \frac{\partial F_d}{\partial s} = 0 \tag{50}$$

Let $\theta_s = \frac{\partial\theta}{\partial s}$. Then

$$\begin{aligned} dF_d(\theta,\theta_s) &= \frac{\partial F_d}{\partial\theta} d\theta + \frac{\partial F_d}{\partial \theta_s} d\theta_s \\ &= \left(\frac{\partial F_d}{\partial\theta}\frac{\partial\theta}{\partial s} + \frac{\partial F_d}{\partial\theta_s}\frac{\partial\theta_s}{\partial s}\right) ds \\ &= \frac{\partial F_d}{\partial s} ds \\ &= 0 \end{aligned}$$

Thus $F_d = C$ is constant and $C = \frac{1}{2} G \left(\frac{\partial\theta}{\partial s}\right)^2$ can be written in the form of Eq. (42) and integrated to obtain Eq. (46).

As in the one-dimensional case, the surface energy, W_1, can now be written in terms of the sample thickness, d, and the tilt angles θ_1 and θ_2. The first step is to derive the equilibrium conditions for the balance of torques at the surface from Eq. (18). Consider the first integral in Eq. (18), viz.,

$$\iiint \left[\frac{\partial}{\partial x}\left(\frac{\partial F_d}{\partial \theta_x}\,\delta\theta\right) + \frac{\partial}{\partial z}\left(\frac{\partial F_d}{\partial \theta_z}\,\delta\theta\right)\right] dxdydz$$

Using $\theta_x = a\theta_z$ and taking the indicated derivatives, the integrand becomes

$$\frac{\partial}{\partial x}\left(\frac{\partial F_d}{\partial \theta_x}\,\delta\theta\right) + \frac{\partial}{\partial z}\left(\frac{\partial F_d}{\partial \theta_z}\,\delta\theta\right) = \frac{\partial}{\partial z}\,(G\theta_z)\delta\theta + (G\theta_z)\,\frac{\partial}{\partial z}\,(\delta\theta) = \frac{\partial}{\partial z}\,(G\theta_z\delta\theta) \tag{51}$$

The first integral in Eq. (18) is then

$$\iint \left[\int_{z_1}^{z_2} \frac{\partial}{\partial z}\,(G\theta_z\delta\theta)dz\right] dxdy = \iint \left[G\theta_z\delta\theta\right]_{z_1}^{z_2} dxdy \tag{52}$$

Using the lower limit in Eq. (52), the total variation of the surface terms at the lower surface is given by

$$-\iint \left[G\theta_z\delta\theta\right]_{z=z_1} dxdy + \iint \delta\,\omega_1 dxdy$$

$$= \iint \left\{\left[-G\theta_z + W_1\sin(2(\theta - \phi_1))\right]\delta\theta\right\}_{z=z_1} dxdy$$

$$= 0 \tag{53}$$

Eq. (53) yields the equilibrium condition for the balance of torques at the lower surface, viz.,

$$G\theta_z\big|_{z=z_1} = W_1\sin[2(\theta_1 - \phi_1)] \tag{54}$$

Substituting $G\theta_z = (2CG)^{1/2}$ and $2C = \dfrac{\left[E_2(\theta_1,\theta_2)\right]^2}{d^2}$, we obtain for the surface energy at the lower surface

$$W_1 = \frac{(G^{1/2})_{\theta=\theta_1} E_2(\theta_1,\theta_2)}{d\,\sin[2(\theta_1 - \phi_1)]} \tag{55}$$

which for $a = 0$ becomes identical to the one-dimensional result given by Eq. (31).

RESULTS AND DISCUSSION

Equations for the surface anchoring energy have been derived for two cases which allow for elastic anisotropy, i.e., $K_1 \neq K_3$. These equations, including the one-dimensional isotropic result of RLG, are summarized in Table I below.

TABLE I. Surface anchoring energies, W_1, for isotropic and anisotropic elasticity.

	W_1	
One-dimension isotropic $K = K_1 = K_3$	$\dfrac{K(\theta_2 - \theta_1)}{d \sin[2(\theta_1 - \theta_1)]}$	Eq. (6)
One-dimension anisotropic $K_1 \neq K_3$	$\dfrac{(g_3^{1/2})_{\theta=\theta_1} E1(\theta_1,\theta_2)}{d \sin[2(\theta_1 - \phi_1)]}$	Eq. (31)
Two-dimension anisotropic $K_1 \neq K_3$	$\dfrac{(G^{1/2})_{\theta=\theta_1} E_2(\theta_1,\theta_2)}{d \sin[2(\theta_1 - \phi_1)]}$	Eq. (55)

The quantities g_3, $E_1(\theta_1,\theta_2)$, G and $E_2(\theta_1,\theta_2)$ in Table I are defined by Eqs. (11), (25), (37) and (45), respectively.

For numerical comparison of elastic anisotropy effects on the calculated values of W_1, it suffices to use only the numerators of the

expressions given in Table I. Of the elastic constants, the bend constant is the more sensitive indicator of elastic anisotropy, particularly near the nematic-smectic A transition. To emphasize the dependence on K_3, the numerators are rewritten as follows.

$$(g_3^{1/2})_{\theta=\theta_1} E_1(\theta_1,\theta_2) = K_3(\underline{g}_3^{1/2})_{\theta=\theta_1} \underline{E}_1(\theta_1,\theta_2) \tag{56}$$

where $\underline{g}_3 = \frac{1}{K_3} g_3 = (1 + k \cos^2\theta)$

$$\underline{E}_1(\theta_1,\theta_2) = \frac{1}{K_3} E_1(\theta_1,\theta_2) = \int_{\theta_1}^{\theta_2} \underline{g}_3^{1/2} d\theta$$

and $k = \frac{K_1}{K_3} - 1$. Also

$$(\underline{G}^{1/2})_{\theta=\theta_1} E_2(\theta_1,\theta_2) = K_3(\underline{G}^{1/2})_{\theta=\theta_1} \underline{E}_2(\theta_1,\theta_2) \tag{57}$$

where $\underline{G} = \frac{1}{K_3} G = \left[(1 + a^2) + k(\cos\theta + a \sin\theta)^2\right]$

$$\underline{E}_2(\theta_1,\theta_2) = \frac{1}{K_3} E_2(\theta_1,\theta_2) = \int_{\theta_1}^{\theta_2} \underline{G}^{1/2} d\theta$$

Equations (56) and (57), representing the one- and two-dimensional anisotropic cases, are to be compared with $K(\theta_2 - \theta_1)$. Evaluation of W_1 as shown requires knowledge of θ_1, θ_2 and d. The slightly wedge-shaped sample configuration used by RLG (Ref. 7) did not allow simultaneous accurate measurement of both θ_1 and θ_2. To enable evaluation of W_1 from measured values of θ_1 and d only, RLG made the assumption mentioned in the Introduction, namely that $(\theta_2 - \theta_1) \cong (\phi_2 - \phi_1) = \Delta\phi$

remained approximately constant over the region of measurement. Eq. (6) for W_1 then becomes

$$W_1 = \frac{K\Delta\phi}{d \sin[2(\theta_1 - \phi_1)]} \tag{58}$$

The above assumption also predicted the experimentally observed approximately linear variation of θ_1 with $1/d$. This linear dependence is readily seen by rewriting Eq. (58) as follows, using $\sin[2(\theta_1 - \phi_1)] \tilde{=} 2(\theta_1 - \phi_1)$ for small angles $(\theta_1 - \phi_1)$.

$$\theta_1 = \left(\frac{K\Delta\phi}{2W_1}\right)\frac{1}{d} + \phi_1 \tag{59}$$

For numerical evaluation of Eqs. (56) and (57), the assumption guiding the choice of θ_1 and θ_2 is that θ_1 vary linearly with $1/d$ for small angles $(\theta_1 - \phi_1)$. Equations (56) and (57) should then remain constant. The surface anchoring energy in the one-dimensional isotropic case (Ref. 7) was evaluated using $\phi_1 \sim 30^o$ and $\phi_2 \sim 90^o$ for θ_1 and θ_2, respectively. The same procedure is followed to enable a numerical evaluation for the anisotropic cases presented here. The calculated values of Eqs. (56) and (57) are presented in Table II for a range of anisotropic conditions, from the isotropic elastic case where $K = K_1 = K_3$ to large anisotropy where $K_3 = 10\ K_1$. For comparison purposes, it was assumed $K = K_1 = 1$, with K_3 allowed to vary.

It was shown previously that $|a| \lesssim \tan\alpha$. For the purposes of numerical evaluation, it was assumed that $a = -\tan\alpha$. For α equal to 18 minutes of arc, $\tan\alpha = 5.24\text{x}10^{-3}$. Because of the smallness of this

TABLE II. Numerical evaluation of Eqs. (56) and (57) and comparison with $K\Delta\phi$.

K_3/K_1	1	1.5	2	5	10
$k = \frac{K_1}{K_3} - 1$	0	-0.333	-0.5	-0.8	-0.9
$K\Delta\phi$	60.0	--	--	--	--
$\underline{g}_3^{1/2}\Big\|_{\theta=\phi_1}$	1.0	0.866	0.791	0.633	0.570
$\underline{E}_1(\phi_1,\phi_2)$	60.0	56.92	55.29	52.05	50.87
$\underline{g}_3^{1/2}\Big\|_{\theta=\phi_1}\underline{E}_1$	60.0	49.30	43.71	32.92	29.00
$K_3\left(\underline{g}_3^{1/2}\right)_{\theta=\phi_1}\underline{E}_1$	60.0	73.95	87.42	164.6	290.0
$\underline{G}^{1/2}\Big\|_{\theta=\phi_1}$	1.0	0.867	0.792	0.635	0.574
$\underline{E}_2(\phi_1,\phi_2)$	60.0	56.98	55.35	52.16	51.00
$\underline{G}^{1/2}\Big\|_{\theta=\phi_1}\underline{E}_2$	60.0	49.41	43.84	33.14	29.26
$K_3\left(\underline{G}^{1/2}\right)_{\theta=\phi_1}\underline{E}_2$	60.0	74.11	87.68	165.7	292.6
$\frac{K_3\left(\underline{g}_3^{1/2}\right)_{\theta=\phi_1}\underline{E}_1}{K\Delta\phi}$	1.0	1.23	1.46	2.74	4.83

factor, the two-dimensional results shown in Table II do not differ significantly from the one-dimensional anisotropic results and hence will not be discussed further.

As Table II shows, anisotropy effects are significant. Whereas, both $\underline{g}_3$ and $\underline{E}_1(\theta_1,\theta_2)$ decrease with increasing K_3, the overall effect resulting from the factor K_3 is an increase in the calculated values of W_1. The ratios of W_1 for the anisotropic case to W_1 for the isotropic case range from 1.23 for $K_3 = 1.5\ K_1$ up to 4.83 for $K_3 = 10\ K_1$.

The above calculations show that inclusion of elastic anisotropy effects can contribute significantly to values of the surface anchoring energy calculated from measurements of surface tilt angles. In the experiment with the wedge-shaped sample (Ref. 7), lack of knowledge of θ_2 hindered including elastic anisotropy effects directly in the calculation of surface energies, although one can assume an average of K_1 and K_3 for the value of K. The liquid crystal used in this experiment (Ref. 7) was 4-cyano-4'n-hexylbiphenyl (6CB) whose elastic constants have a ratio of about $K_3/K_1 = 2$ at room temperature. Table II shows that at $K_3 = 2K_1$, the anisotropy effect could cause almost a 50% difference in the calculated value of the anchoring energy.

It would be desirable to rigorously include anisotropy effects in the calculation of W_1. An experiment is now described which permits this and uses the exact one-dimensional equation for W_1 (Eq. (31)). The sample configuration for this experiment consists of two parallel surfaces where the nematic layer is of constant thickness, d, over the sample. The experimental technique of RLG (Refs. 7 and 8) is used to

measure the director tilt angles (θ_1 and θ_2) at both surfaces. As described in the Introduction, the RLG technique consisted of deducing θ_1 from reflectivity measurements at the critical angle of parallel polarized light from a laser light source. This technique is capable of detecting very small variations in liquid crystal orientation at the substrate surface. Tilt angles were measured to within ± 0.3 degrees. A glass prism of high index of refraction (about 1.9) was used for the lower substrate. In the experiment being proposed, use of a glass prism with appropriate index of refraction would enable measurement of θ_2 at the upper surface as well. Both θ_1 and θ_2 could then be measured at a number of locations over the sample and statistically averaged to obtain representative values for the surfaces. An advantage of the proposed experimental approach is that, by measuring both θ_1 and θ_2, no approximations need be made in the calculation of the surface anchoring energy. Elastic anisotropy would be directly accounted for. The only assumption, which is necessary in any case, is the surface energy model in Eq. (1).

The proposed experimental technique is potentially useful for the systematic determination of surface anchoring energies, strong and weak, for a variety of surface treatments and nematic materials. Such knowledge could contribute to both a better understanding of liquid crystal-substrate interactions and the development of liquid crystal display technology.

REFERENCES

1. Goodman, L. A., "Liquid Crystal Displays - Packaging and Surface Treatments," RCA Rev., 35, 447 (1974); and Kahn, F. J., Taylor, G. N., and Schonhorn, H., "Surface Produced Alignment of Liquid Crystals," Proc. IEEE, 61, 823 (1973).

2. Guyon, E. and Urbach, W., "Anchoring Properties and Alignment of Liquid Crystals," in Non-emissive Electrooptic Displays, Kmetz, A. R. and Von Willisen, F. K., Eds. (Plenum Press, New York, 1976).

3. DeGennes, P. G., The Physics of Liquid Crystals (Clarendon Press, Oxford, 1975).

4. Kleman, M. and Williams, C., "Anchoring Energies and the Nucleation of Surface Disclination Lines in Nematics," Phil. Mag., 28, 725 (1973); and Ryschenkov, G. and Kleman, M., "Surface Defects and Structural Transitions in Very Low Anchoring Energy Nematic Thin Films" J. Chem. Phys., 64, 404 (1976).

5. Naemura, S., "Measurement of Interfacial Interactions Between a Nematic Liquid Crystal and Various Substrates," Appl. Phys. Lett., 33, 1 (1978).

6. Sicart, J., "Method for Measuring the Anchoring Energy of a Nematic," J. Physique Lett., 37, L-25 (1976).

7. Rivière, D., Lévy, Y., and Guyon, E., "Determination of Anchoring Energies from Surface Tilt Angle Meaurements in a Nematic Liquid Crystal," J. Physique Lett., 40, L-215 (1979).

8. Lévy, Y., Rivière, D., Imbert, C. and Boix, M., "Determination of Orientation Angles of a Nematic Liquid Crystal in the Vicinity of the Substrate," Optics Comm., 25, 225 (1978).

9. Sheng P., "Introduction to the Elastic Continuum Theory of Liquid Crystals," in Introduction to Liquid Crystals, Priestley, E. B., Wojtowicz, P. J. and Sheng, P., Eds. (Plenum Press, New York, 1974).

10. Forsyth, A. R., Theory of Differential Equations, Part IV - "Partial Differential Equations," Vol. VI (Dover Pub., New York, 1959), and Nonlinear Partial Differential Equations; a Symposium on Methods of Solution, Ames, W. F., Ed. (Academic Press, New York, 1967).

11. Sneddon, I. N., Elements of Partial Differential Equations (McGraw-Hill, New York, 1957).

1. Report No.	2. Government Accession No.	3. Recipient's Catalog No.
NASA TM-81628		

4. Title and Subtitle	5. Report Date
THEORETICAL MODEL APPLICABLE TO THE EXPERIMENTAL DETERMINATION OF SURFACE ANCHORING ENERGIES OF NEMATIC LIQUID CRYSTALS	November 1980
	6. Performing Organization Code 506-55
7. Author(s) Edwin G. Wintucky	8. Performing Organization Report No. E-637
	10. Work Unit No.
9. Performing Organization Name and Address National Aeronautics and Space Administration Lewis Research Center Cleveland, Ohio 44135	11. Contract or Grant No.
	13. Type of Report and Period Covered Technical Memorandum
12. Sponsoring Agency Name and Address National Aeronautics and Space Administration Washington, D.C. 20546	14. Sponsoring Agency Code

15. Supplementary Notes
Thesis submitted in partial fulfillment of the requirements for the Degree of Master of Science in Physics at Kent State University, Kent, Ohio.

16. Abstract

For a cell configuration consisting of a thin nematic layer bounded by two parallel plane surfaces, with opposing surfaces suitably treated to produce dissimilar molecular orientations, the elastic continuum theory for nematic liquid crystals has been applied to derive an expression relating surface anchoring energies to elastic constants, director oritentations at the substrate surfaces, and cell thickness. A numerical comparison with the elastically isotropic result over a range $K_3 = 1.5\ K_1$ to $K_3 = 10\ K_1$ showed the effect of elastic anisotropy could be quite significant. Surface anchoring energies calculated for anisotropic of $K_3 = 2\ K_1$ and $K_3 = 10\ K_1$ were approximately 50% and 500% larger, respectively, than the isotropic values.

17. Key Words (Suggested by Author(s))	18. Distribution Statement
Liquid crystals Surface anchoring energies Elastic continuum theory	Unclassified - unlimited STAR Category 70

19. Security Classif. (of this report)	20. Security Classif. (of this page)	21. No. of Pages	22. Price*
Unclassified	Unclassified		

* For sale by the National Technical Information Service, Springfield, Virginia 22161